materials proceedings

MDPI

Proceeding Paper

4-Ammoniumbutylstyrene Based-Nanoparticles for the Controlled Release of Fenretinide †

Guendalina Zuccari [1,*], Eleonora Russo [1], Carla Villa [1], Danilo Marimpietri [2], Alessia Zorzoli [2] and Silvana Alfei [1]

[1] Department of Pharmacy (DiFAR), University of Genoa, Viale Cembrano 4, I-16148 Genova, Italy; russo@difar.unige.it (E.R.); villa@difar.unige.it (C.V.); alfei@difar.unige.it (S.A.)
[2] Cell Factory, IRCCS Istituto Giannina Gaslini, Via Gerolamo Gaslini 5, 16147 Genova, Italy; alessiazorzoli@gaslini.org (D.M.), danilomarimpietri@gaslini.org (A.Z.)
* Correspondence: guendalina.zuccari@unige.it
† Presented at the 4th International Online Conference on Nanomaterials, 5–19 May 2023; Available online: https://iocn2023.sciforum.net.

Abstract: Fenretinide (4-HPR), a synthetic retinoid with low toxicological profile, is endowed with high antitumor activity. However, 4-HPR shows poor oral absorption due to its low solubility, and variable blood concentrations for a massive hepatic first pass effect. Here, we prepared nanoparticles (NPs) made of 4-ammoniunbutylstyrene random copolymer (P5) by the anti-solvent co-precipitation technique. The encapsulation led to an increase in drug apparent solubility of 1134 folds with a drug loading of 37%. The NPs showed an extended dissolution rate, a mean diameter of 249 nm, positive Zeta potential, and confirmed an anti-proliferative activity on neuroblastoma cells.

Keywords: fenretinide; drug delivery; nanoparticles; neuroblastoma

Citation: Zuccari, G.; Russo, E.; Villa, C.; Marimpietri, D.; Zorzoli, A.; Alfei, S. 4-Ammoniumbutylstyrene Based-Nanoparticles for the Controlled Release of Fenretinide. *Mater. Proc.* **2023**, *14*, x. https://doi.org/10.3390/xxxxx
Published: 5 May 2023

1. Introduction

Fenretinide (N-(4-hydroxyphenyl)retinamide (4-HPR), belongs to the third generation of retinoids but its mechanisms of action are quite different from those of retinoic acid [1]. Indeed, 4-HPR is endowed with a more favorable toxicological profile and a better tissue distribution [2]. Unfortunately, the very poor water solubility of 4-HPR constraints the drug plasmatic levels under those effective, consequently, clinical trials showed high variability in results [3]. As a result, new formulations are required to enhance the bioavailability of 4-HPR. In recent years, many attempts have been made to enhance the drug aqueous solubility, including micellar solubilization with amphiphilic dextrins or branched polyethylene glycol [4,5], conjugation with polyvinyl alcohol [6], encapsulation into PLGA microparticles [7], liposomes [8] and lately drug ionization [9]. Here, we employed the anti-solvent co-precipitation process for the preparation of 4-HPR loaded-nanoparticles (4-HPR-P5 NPs) by employing a water-soluble cationic copolymer (P5) obtained by copolymerizing the laboratory-made monomer 4-ammoniumbuthylstyrene hydrochloride with di-methyl-acrylamide (DMAA) as uncharged diluent [10]. This approach could simultaneously achieve the goal of drug amorphization and nanosizing. In this study, we prepared and characterized 4-HPR-P5 NPs and the formulation was tested for its antiproliferative activity against neuroblastoma cells.

2. Materials and Method

2.1. Experimental Procedures to Prepare and Characterized 4-HPR-P5 NPs

The 4-HPR-P5 NPs were prepared by the nanoprecipitation technique. The yellow methanol solution of P5 and 4-HPR was added to the non-solvent phase (diethyl ether) drop-wise, at room temperature and under stirring. A fine dispersion was obtained, which was centrifuged for solvents separation.

FTIR spectra of 4-HPR, recovered 4-HPR (R-4-HPR), P5 and 4-HPR-P5 NPs were recorded in triplicate on samples as KBr pellets in transmission mode using a Spectrum Two FT-IR Spectrometer (PerkinElmer, Inc., Waltham, MA, USA).

To assess the drug loading content% (DL%) of solid 4-HPR-P5 NPs, the powder obtained was dissolved in MeOH to assay the drug concentration by UV-Vis spectrophotometric analysis at λ_{max} = 364 nm (HP 8453, Hewlett Packard, Palo Alto, CA, USA). The DL% was calculated according to the formula in Equation (1).

$$\mathrm{DL\%} = \frac{\text{wheight of drug in the loaded NPs}}{\text{wheight of the solid NPs}} \times 100 \quad (1)$$

The water solubility of solid 4-HPR-P5 NPs was performed by adding increasing amounts of powder to 10 mL of water in a sealed vial until a precipitate was obtained. Replicated samples were maintained at 25 °C under stirring in an incubator and after 24 h filtered using a 0.22 μm filter and assayed for drug content by UV-Vis analysis. The stability of the supersaturated solutions (1,2,4 mg/mL) were investigated by storing the colloidal dispersions at 25 °C and visually observed after 24, 48 and 72 h for signs of precipitation.

To confirm the amorphization of 4-HPR inside the nanoparticles, DSC analysis was performed (TA Instrument, New Castle, DE, USA).

Particle size (Z-average), polydispersity index (PDI) and Zeta potential (ʒ) of colloidal suspensions were measured using a Malvern Nano ZS90 light scattering apparatus (Malvern Instruments Ltd., Worcestershire, UK). The ʒ potential values of micelles were recorded in distilled water.

The in vitro studies were carried in phosphate buffer solution (PBS) pH 7.4 at 37 °C. An amount of 4-HPR-P5 NPs powder was reconstituted with 5 mL of PBS and filled in a dialysis tube and then dialyzed against 50 mL of isotonic PBS and 10 mL of chloroform. A corresponding 4-HPR raw powder was suspended in the same volume to have an equal drug concentration and tested along with the loaded NPs. At fixed time intervals chloroform was removed, evaporated and the residue was dissolved in 300 μL of acetonitrile and analysed by RP-HPLC DAD to determine the amount of drug released over time (Hewlett-Packard HP1100, Palo Alto, CA, USA).with a mobile phase of CH_3CN:H_2O:CH_3COOH (80:18:2, *v*/*v*/*v*), flow rate 1 mL/min, absorbance detector set at 360 nm.

To assay cell proliferation under 4-HPR exposure, human neuroblastoma cell lines, IMR-32 and SH-SY5Y were seeded in triplicate in a 96w plate, from 3000 to 10,000 cells for well in 200 μL of complete medium. After 24 h the medium was changed and the cells were exposed for 24, 48, or 72 h to free 4-HPR at 0.1, 0.5, 1, 2, 5, 7.5, 10, 15 μM), 4-HPR-P5 NPs in concentrations able of providing the same concentrations of free 4-HPR, and P5 at the concentrations provided by the amounts of 4-HPR-P5 NPs tested. The effect on cell growth was evaluated by a fluorescence-based proliferation and cytotoxicity assay (CyQUANT® Direct Cell Proliferation Assay, Thermo Fisher Scientific, Life Technologies, MB, Italy)

2.2. Statistical Analysis

All the experiments were performed at least three times. Differential findings among the experimental groups were determined by two-way ANOVA analysis of variance, with Bonferroni posttests, using GraphPad Prism 5 (GraphPad Software v5.0, San Diego, CA, USA). Asterisks indicate the following *p*-value ranges: * = $p < 0.05$, ** = $p < 0.01$, *** = $p < 0.001$.

3. Results and Discussion

3.1. Preparation and Characterization of 4-HPR-P5 NPs

An aqueous phase is mostly used as anti-solvent to precipitate the drug/polymer complex, but, since P5 was soluble in water, the aqueous phase was replaced by Et_2O, in which P5 was insoluble and 4-HPR poorly soluble. MeOH was chosen to solubilize both P5 and 4-HPR. The addition of the methanol solution containing P5 and 4-HPR to the non-solvent under moderate stirring led to nucleation and to the formation of a precipitate. Figure 1 shows the FTIR spectrum of 4-HPR-P5 NPs, where bands belonging to both P5 (2926, 1617, 1259, 1132 and 1060 cm^{-1}) and the entrapped 4-HPR (2633, 2529, 1512, and 827 cm^{-1}) can be detected.

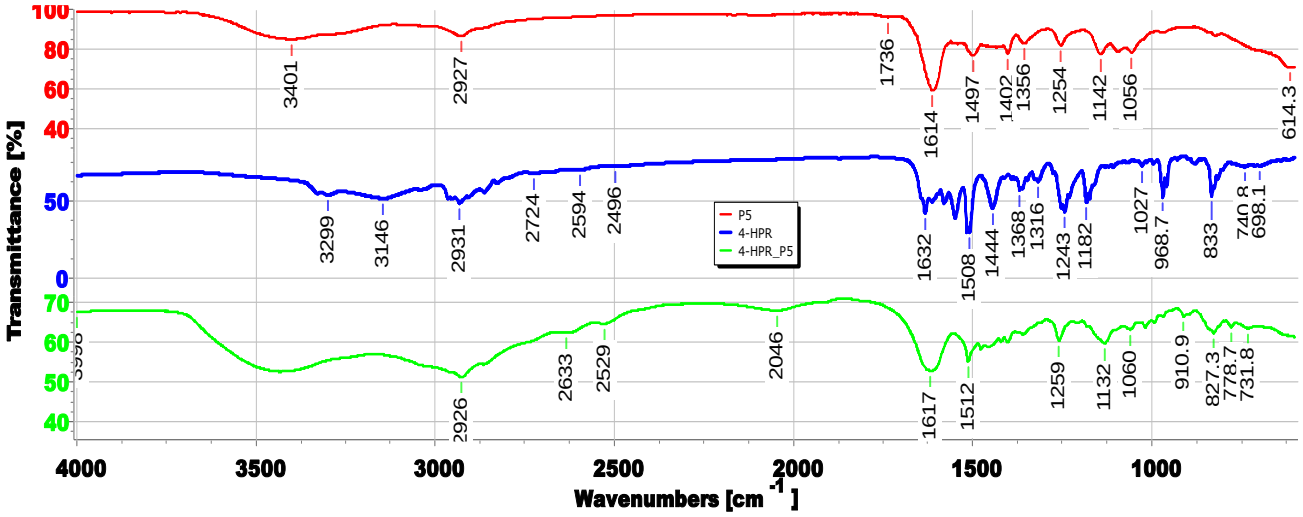

Figure 1. FTIR spectra of 4-HPR-P5 NPs (green line), P5 (red line) and pristine 4-HPR (blue line) for easier comparison.

The DL% was found to be 37 ± 3.46%. The high value suggests the formation of strong interactions between the drug and the copolymer and their repulsion for the anti-solvent. The total drug solubility estimated from a 4-HPR-P5 saturated solution corresponded to 1.94 ± 0.68 mg/mL which represents a 1134-fold increase with respect to the pure drug (1.17 μg/mL). This value is significantly higher in comparison to conjugates with polyvinyl alcohol (343 μg/mL), amphiphilic PVA based micelles (111 μg/mL) and is comparable with those obtained with polymeric micelles made of amphiphilic dextrins (2.8 mg/mL) or branched polyethylene glycol (1.72 mg/mL). To assess the stability of the colloidal suspensions, different 4-HPR-P5 NPs concentrations, ranging from 1 to 4 mg/mL, were kept in water in an incubator at 25 °C, and after three days, the samples were microscopically inspected to detect the formations of precipitates and assayed for drug content in solution. No statistically significant differences were found in the period considered.

DSC thermograms of the 4-HPR-P5 NP powder, in comparison to the corresponding physical mixture, as well as to raw 4-HPR and P5, are depicted in Figure 2. The 4-HPR thermogram showed the characteristic endothermic peak at 174.23 °C due to 4-HPR's melting point. P5 showed a broad endotherm corresponding to copolymer dehydration due to the numerous protonated amine groups which made the material highly hydroscopic. The physical mixture profile confirmed the presence of the copolymer dehydration and a quite evident melting peak of the drug. 4-HPR-P5 NPs profile appeared remarkably different, evidencing the disappearing of 4-HPR melting peak, indicative of the absence of the drug in the crystalline state. Moreover, also the broad initial peak disappeared suggesting that high lipophilic drug molecules dispersed within the polymeric chains reduce P5 tendency to adsorb humidity.

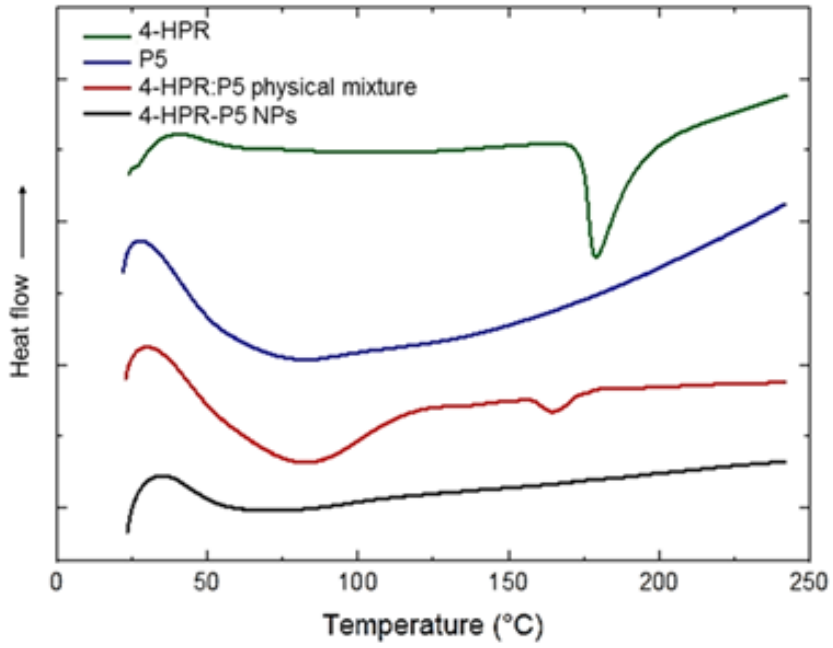

Figure 2. DSC thermograms of raw 4-HPR, P5, 4-HPR:P5 physical mixture, and 4-HPR-P5 NPs.

In Figure 3 representative size distributions and Zeta potential are reported.

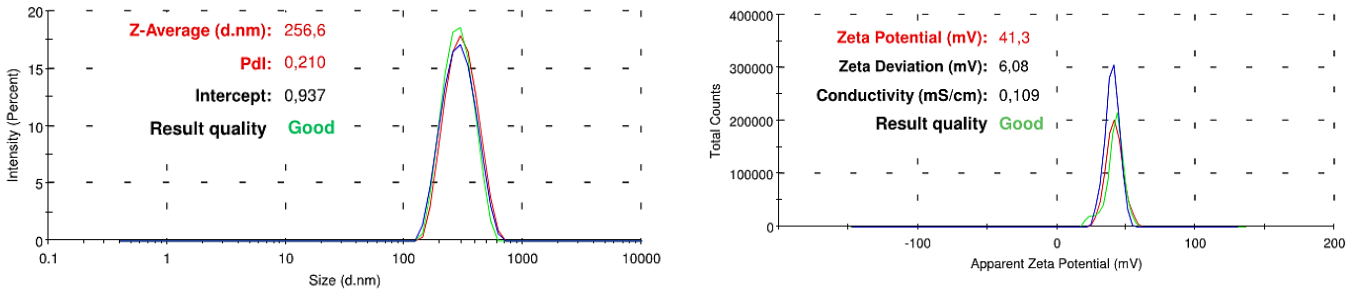

(**a**) (**b**)

Figure 3. (**a**) Representative size distribution of 4-HPR-P5 NPs, and (**b**) representative Zeta potential obtained by dissolving 2 mg/mL of nanoparticles, measured in water at 25 °C.

Size analysis confirmed the suitability of 4-HPR-P5 NPs to freely extravasate through the capillary discontinuity of the tumour tissue, thus improving the therapeutic efficacy of 4-HPR by the EPR effect.

The release profile highlighted the strong interactions between the copolymer and the drug, since NPs have not delivered all their cargo in the time period considered. As depicted in Figure 4, a sustained drug release has been observed, with a fractional release at 48 h of 38.7% ± 1.5%.

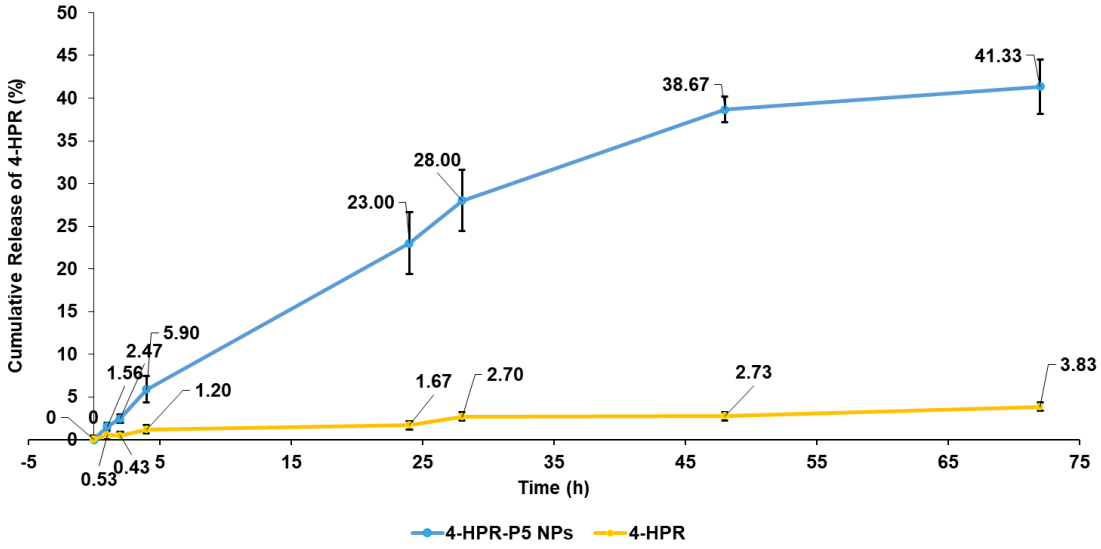

Figure 4. CR% of 4-HPR from NPs and from its suspension at pH 7.4, monitored for 72 h.

The amorphous drug dissolves much more rapidly than the crystalline form in aqueous solution due to the combined effects of a lack of crystalline lattice and the elevated water solubility of the copolymer, leading to a supersaturated drug concentration.

3.2. Cytotoxic Activity of 4-HPR and 4-HPR-P5 NPs on Neuroblastoma Cell Lines

Dose- and time-dependent cytotoxicity experiments were performed to evaluate the effects of HPR-P5 NPs on IMR-32 and SH-SY5Y neuroblastoma cells. The concentrations of each sample administered to cells have been detailed in Table 1.

Table 1. Concentrations of each sample administered to NB cells.

Samples	Concentrations (μM)							
HPR	0.1	0.5	1	2	5	7.5	10	15
HPR-P5	0.0132	0.0655	0.1310	0.2620	0.6551	0.9827	1.3100	1.9654
P5	0.0130	0.0650	0.1300	0.2600	0.6500	0.9803	1.3000	1.9606

The IC50 for all samples were reported in Table 2.

Table 2. IC50 of 4-HPR, P5 and 4-HPR-P5 NPs towards IMR-32 and SH-SY5Y NB cells at 24, 48 and 72 h.

Cells	Times (h)	4-HPR (μM)	P5 (μM)	4-HPR-P5 NPs (μM)
IMR-32	24	1.08	N.D.	1.07
	48	1.93	N.D.	1.76
	72	0.68	N.D.	1.25
SH-SY5Y	24	7.84	N.D.	N.D.
	48	4.32	N.D.	N.D.
	72	4.99	N.D.	1.93

N.D. = not detected.

4. Conclusions

We succeeded in preparing a powder formulation of Fenretinide molecularly dispersed and entrapped within the hydrophilic scaffold of P5, by employing the anti-solvent co-precipitation technique. We used as solvent (MeOH) and as anti-solvent (Et_2O), having both boiling points, which allowed an easy isolation of the product without its exposure to high temperatures. The amorphization was confirmed by thermal studies and the high

payload reached determined an increase of the drug apparent solubility of 1134 folds. The in vitro antiproliferative activity observed for 4-HPR-P5 was in agreement with the slow release of drug from t the formulation, while the calculated IC50 values were comparable or even lower than those of free 4-HPR.

Author Contributions: Conceptualization, G.Z.; methodology, G.Z. and S.A.; validation and formal analysis, G.Z.; investigation, E.R., C.V., G.Z., S.A., D.M. and A.Z.; data curation, G.Z. and S.A.; writing—original draft preparation, G.Z.; writing—review and editing, G.Z., S.A., C.V., E.R. and D.M.; supervision G.Z., S.A. All authors have read and agreed to the published version of the manuscript.

Funding: This research received no external funding.

Institutional Review Board Statement: Not applicable.

Informed Consent Statement: Not applicable.

Data Availability Statement: All data concerning this study are contained in the present manuscript or in previous articles whose references have been provided.

Conflicts of Interest: The authors declare no conflict of interest.

References

1. Sporn, M.B.; Dunlop, N.M.; Newton, D.L.; Henderson, W.R. Relationships between Structure and Activity of Retinoids. *Nature* **1976**, *263*, 110–113. https://doi.org/10.1038/263110a0.
2. Cooper, J.P.; Reynolds, C.P.; Cho, H.; Kang, M.H. Clinical Development of Fenretinide as an Antineoplastic Drug: Pharmacology Perspectives. *Exp. Biol. Med*. **2017**, *242*, 1178–1184. https://doi.org/10.1177/1535370217706952.
3. Villablanca, J.G.; London, W.B.; Naranjo, A.; McGrady, P.; Ames, M.M.; Reid, J.M.; McGovern, R.M.; Buhrow, S.A.; Jackson, H.; Stranzinger, E.; et al. Phase II Study of Oral Capsular 4-Hydroxyphenylretinamide (4-HPR/Fenretinide) in Pediatric Patients with Refractory or Recurrent Neuroblastoma: A Report from the Children's Oncology Group. *Clin. Cancer Res.* **2011**, *17*, 6858–6866. https://doi.org/10.1158/1078-0432.CCR-11-0995.
4. Orienti, I.; Zuccari, G.; Carosio, R.; Montaldo, P.G. Improvement of Aqueous Solubility of Fenretinide and Other Hydrophobic Anti-Tumor Drugs by Complexation with Amphiphilic Dextrins. *Drug Deliv.* **2009**, *16*, 389–398. https://doi.org/10.1080/10717540903101655.
5. Orienti, I.; Zuccari, G.; Falconi, M.; Teti, G.; Illingworth, N.A.; Veal, G.J. Novel Micelles Based on Amphiphilic Branched PEG as Carriers for Fenretinide. *Nanomed. Nanotechnol. Biol. Med.* **2012**, *8*, 880–890. https://doi.org/10.1016/j.nano.2011.10.008.
6. Orienti, I.; Zuccari, G.; Bergamante, V.; Carosio, R.; Gotti, R.; Cilli, M.; Montaldo Fenretinide-Polyvinylalcohol Conjugates: New Systems Allowing Fenretinide Intravenous Administration. *Biomacromolecules* **2007**, *8*, 3258–3262. https://doi.org/10.1021/bm7005592.
7. Zhang, Y.; Wischke, C.; Mittal, S.; Mitra, A.; Schwendeman, S.P. Design of Controlled Release PLGA Microspheres for Hydrophobic Fenretinide. *Mol. Pharm.* **2016**, *13*, 2622–2630. https://doi.org/10.1021/acs.molpharmaceut.5b00961.
8. Di Paolo, D.; Pastorino, F.; Zuccari, G.; Caffa, I.; Loi, M.; Marimpietri, D.; Brignole, C.; Perri, P.; Cilli, M.; Nico, B.; et al. Enhanced Anti-Tumor and Anti-Angiogenic Efficacy of a Novel Liposomal Fenretinide on Human Neuroblastoma. *J. Control. Release* **2013**, *170*, 445–451. https://doi.org/10.1016/j.jconrel.2013.06.015.
9. Orienti, I.; Salvati, V.; Sette, G.; Zucchetti, M.; Bongiorno-Borbone, L.; Peschiaroli, A.; Zolla, L.; Francescangeli, F.; Ferrari, M.; Matteo, C.; et al. A Novel Oral Micellar Fenretinide Formulation with Enhanced Bioavailability and Antitumour Activity against Multiple Tumours from Cancer Stem Cells. *J. Exp. Clin. Cancer Res.* **2019**, *38*, 373. https://doi.org/10.1186/s13046-019-1383-9.
10. Alfei, S.; Piatti, G.; Caviglia, D.; Schito, A.M. Synthesis, Characterization, and Bactericidal Activity of a 4-Ammoniumbuthylstyrene-Based Random Copolymer. *Polymers* **2021**, *13*, 1140. https://doi.org/10.3390/polym13071140.